

Heterogeneous Ice Nucleation on Simulated Secondary Organic Aerosol

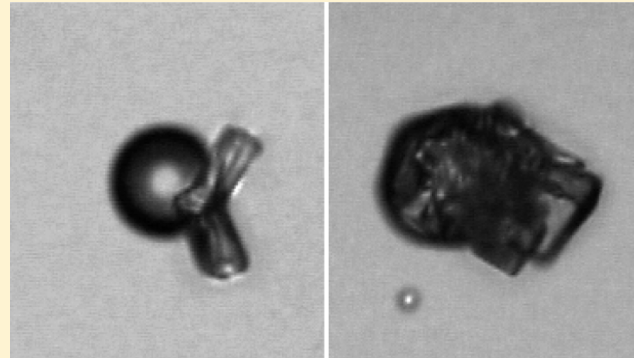
Gregory P. Schill,[†] David O. De Haan,[‡] and Margaret A. Tolbert*,[†]

[†] Cooperative Institute for Research in Environmental Sciences and Department of Chemistry and Biochemistry, University of Colorado, Boulder, Colorado 80309, United States

[‡] Department of Chemistry and Biochemistry, University of San Diego, San Diego, California 92110, United States

Supporting Information

ABSTRACT: In this study, we have explored the phase behavior and the ice nucleation properties of secondary organic aerosol made from aqueous processing (aqSOA). AqSOA was made from the dark reactions of methylglyoxal with methylamine in simulated evaporated cloud droplets. The resulting particles were probed from 215 to 250 K using Raman spectroscopy coupled to an environmental cell. We find these particles are in a semisolid or glassy state based upon their behavior when exposed to mechanical pressure as well as their flow behavior. Further, we find that these aqSOA particles are poor depositional ice nuclei, in contrast to previous studies on simple mixtures of glassy organics. Additionally, we have studied the effect of ammonium sulfate on the phase, morphology, and ice nucleation behavior of the aqSOA. We find that the plasticizing effect of ammonium sulfate lowers the viscosity of the aqSOA, allowing the ammonium sulfate to effloresce within the aqSOA matrix. Upon humidification, the aqSOA matrix liquefies before it can depositionally nucleate ice, and the effloresced ammonium sulfate can act as an immersion mode ice nucleus. This change in the mode of nucleation is accompanied by an increase in the overall ice nucleation efficiency of the aqSOA particles.



INTRODUCTION

Ice clouds are ubiquitous in the upper troposphere (UT) and affect climate by scattering solar and terrestrial radiation and absorbing terrestrial radiation. Despite their ubiquity, ice clouds are poorly constrained in climate models; for example, in their Fourth Assessment, the International Panel on Climate Change did not include an aerosol indirect effect contribution from ice clouds due to an insufficient understanding of ice nucleation by atmospheric aerosol.¹ One reason for this poor understanding is that the chemical nature of ice nuclei (IN) found in the UT is not well constrained. Further, the phases and morphologies of the IN are entirely unknown.

Recently, Froyd et al. utilized a counter-flow virtual impactor coupled to a single particle mass spectrometer to determine the chemical composition of UT background aerosol² and aerosol that nucleated into subvisible cirrus particles.³ In both cases, the dominant aerosol types were mixtures of organics and sulfates; surprisingly, the subvisible cirrus residues did not contain a large number of particles that are typically thought to be excellent IN, such as mineral dust. While the ice nucleation properties of effloresced ammonium sulfate particles are well-known,^{4–6} the effect of adding organic species is uncertain.

Several laboratory studies have shown that coating efficient IN with organic species can deactivate those IN. For example, Mohler et al.⁷ found that coating mineral dust with secondary

organic material from the dark ozonolysis of α -pinene required higher ice supersaturations to nucleate ice compared to the bare dust particle. A recent study from our group has discovered that the phase of the organic coating plays a critical role in determining the ice nucleation ability of effloresced ammonium sulfate particles coated with an organic species.⁸ In that study, we found that if the organic coating is liquid, then the organic material minimally affected the ice nucleation properties of ammonium sulfate; if the coating became sufficiently viscous, however, then the organic coating dictated the ice nucleation properties of the particle. This behavior was attributed to the fast and slow diffusion of water through the liquid and viscous organic coatings, respectively. Several studies have recently shown that soluble organic species can undergo a glass transition under atmospheric conditions^{9,10} and that those organic glasses can nucleate ice heterogeneously;^{11–13} however, fewer studies have looked at the phase behavior and ice nucleation properties of complex secondary organic aerosol. To the authors' knowledge, only one previous study has examined the heterogeneous ice nucleation behavior of pure, glassy

Received: October 20, 2013

Revised: January 6, 2014

Accepted: January 10, 2014

Published: January 10, 2014



secondary organic aerosol, which was generated from the gas phase photooxidation of naphthalene in a Potential Aerosol Mass chamber.¹⁴ In a separate study, it has been shown that this reaction can produce highly viscous semisolid or glassy particles.¹⁵

In addition to the condensation of compounds formed via gas-phase oxidation, secondary organic aerosol can be formed from aqueous reactions in cloud droplets and aqueous aerosol (aqSOA).¹⁶ In fact, recent modeling work has shown that this aqSOA could contribute almost as much organic aerosol by mass as gas-phase oxidation of aerosol precursors (gasSOA).¹⁷ It has been shown that one pathway to aqSOA is via dark reactions between small α -dicarbonyls and reduced amines in evaporating cloud droplets.^{18–20} These reactions are often accompanied by browning and oligomer formation, producing hundreds to thousands of distinct peaks in their electrospray mass spectra; products include imines, imidazoles, and their respective oligomeric products. These high molecular weight products are likely to promote glass formation, as a literature compilation by Koop et al.¹⁰ found glass formation temperature and molecular weight to be highly correlated.

In this work, we have studied the phase behavior and ice nucleation properties of simulated evaporated cloud droplets containing methylglyoxal and methylamine. We find that these simulated evaporated cloud droplets are in a semisolid to glassy phase state, as indicated by their behavior when exposed to mechanical pressure as well as their flow behavior. Furthermore, we find that they are poor IN, in contrast to previous ice nucleation studies on simple mixtures of glassy organics. In addition, we explored the effect of adding ammonium sulfate to the simulated cloud droplets. We find that adding ammonium sulfate lowers the viscosity of the resulting aqSOA and that it not only changes the mode of nucleation but also increases the overall ice nucleation efficacy of the particle.

■ EXPERIMENTAL SECTION

Raman Microscope. The experimental setup has been described in detail previously.^{6,8} Briefly, a Nicolet Almega XR dispersive Raman spectrometer has been coupled to an Olympus BX51 research grade microscope with 10 \times , 20 \times , 50 \times , and 100 \times capabilities. In addition, the Raman microscope has been outfitted with a Linkam THMS 600 environmental cell that can control the temperature (T) of the sample from –191 to 600 °C. The relative humidity (RH) inside the environmental cell is controlled by mixing dry and wet flows of N₂; the wet flow of N₂ is produced by bubbling dry N₂ through a fritted glass bubbler immersed in high-purity water. The absolute water pressure inside of the cell is measured by a Buck Research CR-1A chilled mirror hygrometer in line with the cell, which has an accuracy of 0.15 K. The RH inside of the cell is determined by taking the ratio of the absolute water pressure as determined by the dew point hygrometer to the equilibrium vapor pressure over water as parametrized by Murphy and Koop.²¹ A Gast diaphragm pump is connected to the back of the hygrometer, ensuring that the flow through the system is maintained at 1 L min^{−1}.

Raman spectra and spectral maps were acquired using a frequency doubled Nd:YAG laser operating at 532 nm. All spectra were obtained using either 50 \times or 100 \times objectives, corresponding to diffraction limited spot sizes of 1.3 and 1.1 μ m and depths of field of 11 and 8 μ m, respectively. Spectra were collected from 150 to 4000 cm^{−1}, with a typical spectral resolution of 2–4 cm^{−1}. Raman line and two-dimensional maps

were collected by obtaining spectra every 1 μ m in the Y and XY directions, respectively.

Sample Preparation. Simulated cloud droplets were prepared by first mixing a solution of 8 mM methylglyoxal and 8 mM methylamine. While such a mixture turns yellow over a period of hours, the solution was always used immediately. The solutions were aspirated into a Meinhard TR-50 glass concentric nebulizer, and the nebulized spray was directed onto a hydrophobically treated fused silica disk. The nebulized droplets were allowed to coagulate into supermicrometer droplets, and the silica disk was immediately transferred to the environmental cell and exposed to ~0% RH at 298 K. Upon drying, the concentration of the reactants increases about 3 orders of magnitude to 5–10 M,¹⁹ driving aqueous reactions and leaving aqSOA particles ~1–40 μ m in lateral diameter.

To study the effect of adding ammonium sulfate to the simulated cloud droplets, a solution of 8 mM methylglyoxal, 8 mM methylamine, and 8 mM ammonium sulfate was nebulized under the exact same conditions as above. These droplets were also immediately transferred to the environmental cell at ~0% relative humidity and 298 K.

Impact-Flow and Deliquescence Experiments. To conduct impact-flow experiments, aqSOA particles were first dried in the environmental cell at 298 K and ~0% RH for at least 10 min. The cell was then opened, and the particles were sandwiched by adding an additional fused silica disc. To minimize influence from the laboratory RH, the particles were protected by a blanket of dry N₂ during this process. Mechanical pressure was applied to the outside of both of the discs; the additional disc was then removed, and the original disc was placed back inside the environmental cell. In concurrence with Murray et al.,²² the mechanical pressure exerted on aqSOA will flatten and splatter liquid particles and shatter semisolid or glassy particles.

In order to ensure that particles in impact-flow experiments did not experience high relative humidities upon opening the cell and sandwiching the particles, impact experiments were conducted on effloresced LiCl particles of a similar size distribution. At 298 K, LiCl has a deliquescence relative humidity of 11.3 ± 0.3%;²³ thus, if the particles flatten or splatter, then the particles experienced an RH ≥ 11.3%. The results of these LiCl impact experiment can be seen in Figure S1. As shown, the effloresced LiCl particles started out roughly spherical and upon impact were shattered. Since the particles shattered, they could not have undergone deliquescence, indicating that the particles experienced an RH < 11.3% upon opening the cell and sandwiching the particles between two discs.

If the aqSOA particles shattered, flow experiments were then conducted at various temperatures by raising the relative humidity over the shattered particles. In each experiment, 1–3 shattered particles were observed under 50 \times magnification. The relative humidity was raised by keeping a constant dew point and steadily decreasing the temperature. Specifically, after the dew point remained stable for at least 10 min, T was reduced at 10 K min^{−1} until RH ≈ 60%. The sample was then cooled at a rate of 0.1 K min^{−1}, corresponding to an RH ramp rate of 0.6% min^{−1}, until the crack(s) in a particle started to wane and/or the edges of the shattered particle began to round. This RH was defined as the Start of Flow RH (RH_{flow}). The T was further dropped until RH ≈ 95%, by which time the particles in this study had fully liquefied and resumed a spherical morphology.

For aqSOA + ammonium sulfate studies, impact experiments could not be conducted because the particles contained crystalline material; here it is not possible with our current setup to determine whether the particles shattered under mechanical pressure due to the crystalline material, the amorphous (semi)solid organic, or both, regardless of the phase of the organic material. For these particles, the deliquescence RH of the crystalline material was determined instead. For deliquescence experiments, the particle was also allowed to sit at 298 K and 0% RH for at least 10 min to ensure that the particle was nominally dry. Deliquescence experiments were then conducted in the exact same manner as the flow experiments, except the visual cue was now the prompt dissolution of the crystalline material. For both flow and deliquescence experiments, at least 3 experiments were performed on 3 separate sample discs.

Ice Nucleation Experiments. For ice nucleation experiments, deposited particles were allowed to sit at 298 K and 0% RH for at least 10 min. The ice saturation ratio ($S_{\text{ice}} = P_{\text{H}_2\text{O}}/\text{VP}_{\text{ice}}$) over each particle was then increased by keeping the dew point constant and steadily decreasing T . In this study, after the dew point remained stable for at least 10 min, T was decreased from 298 K at a rate of 10 K min^{-1} until $S_{\text{ice}} \sim 0.9$. The sample was then cooled at a rate of 0.1 K min^{-1} , corresponding to an S_{ice} ramp rate of 0.01 K min^{-1} , until the onset of ice was observed. For each ice particle formed, a Raman line map of that particle was taken to determine whether the organic portion of the particle had spread out over the ice and, therefore, was in a flowing state. After this initial Raman line map was taken, the ice was sublimed by turning off the flow of wet N_2 , and an additional line map of the particle that nucleated ice was taken.

RESULTS AND DISCUSSION

A 50 \times image of methylglyoxal + methylamine aqSOA can be seen in Figure 1a. As shown, the particles are spherical and show no internal structure, suggesting that they are in an amorphous state. This is expected as previous work by De Haan et al.¹⁹ has shown that dark reactions in simulated evaporated cloud droplets containing methylglyoxal and methylamine form products with varied functional moieties, including imines and imidazoles, and contain hundreds of distinct peaks in their electrospray mass spectra; thus, aqSOA produced from these reactions are unlikely to crystallize. From Figure 1a, however, we are unable to discern if they are liquid or (semi)solid. Figure 1b shows the same particles but after mechanical pressure was applied. Here, the particles have shattered after impact, suggesting that they are in a highly viscous, likely solid (glassy) state. Without dynamic viscosity measurements, however, we cannot discern highly viscous semisolids from glasses. Thus, we will refer to these particles as amorphous (semi)solids. In a separate experiment, the shattered particles were allowed to sit at 298 K and 0% RH for 12 h. In this time period, these particles did not exhibit any visual flow behavior. In a similar experiment, Renbaum-Wolff et al.²⁴ found that gasSOA from the photooxidation of α -pinene could be shattered by a needle under comparable conditions; using an advanced multiphysics software package, they surmised that if the edges of a simulated shattered particle did not flow more than $0.5 \mu\text{m}$ after 8 h, it had a viscosity of $\geq 10^8 \text{ Pa s}$, correlating to a particle that was in the semisolid to glassy range.

A typical image series of an impact-flow experiment can be seen in Figure 2, and the full video record can be seen in the

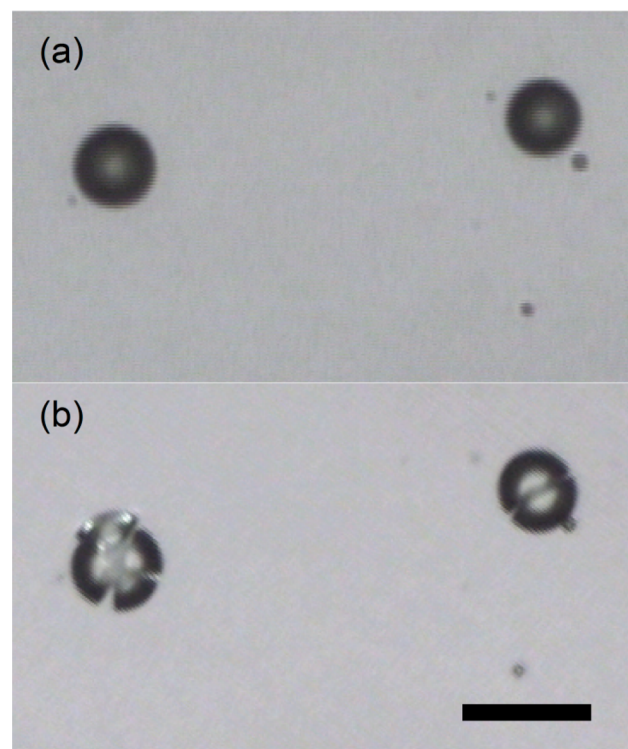


Figure 1. 50 \times image of methylglyoxal + methylamine aqSOA particles (a) freshly dried and (b) immediately after impact. As shown, the amorphous particles shatter under mechanical pressure, indicating that they are in a semisolid or glassy state. The size bar in the bottom right-hand corner corresponds to $20 \mu\text{m}$.

Supporting Information (Movie S1). Through the course of this particular experiment, the RH increases from 51 to 93% as the temperature drops from 253.3 to 246.6 K. As shown, there is no apparent visual change in the particle from Figure 2a to 2b, even though the RH is increasing. At a set RH, however, the edges of the shattered particle start to round (Figure 2c), which we have defined as RH_{flow} . As the RH is increased beyond RH_{flow} , the particle continues to liquefy (Figure 2d) and eventually flows back together into a sphere to reduce the surface tension of the system (Figure 2e). This process occurs because water has a lower viscosity than the aqSOA and, therefore, acts as a plasticizer. It should be noted that full liquefactions will depend on the RH ramp rate and the particle size. While our ramp rates are relevant to the updraft rate of an air parcel in the UT,²⁵ our particles are much larger than particles typically found in the UT.^{2,3} To mitigate this size effect, we have used RH_{flow} , much like Wang et al.¹⁴ and Baustian et al.¹³ used onset water uptake, instead of full liquefaction to indicate a change in flow behavior under our experimental conditions.

The Start of Flow RH, RH_{flow} , for several methylglyoxal + methylamine experiments can be seen in Figure 3. As shown, there is a clear temperature effect, where particles at colder temperatures require higher RH for the edges of the particle to start flowing. A similar trend was shown for the water uptake of glassy SOA made from the gas-phase photooxidation of naphthalene.¹⁴ At 225 K, we could no longer measure RH_{flow} , because at this temperature the semisolid/glassy particles would nucleate ice depositionally first. Thus, at $T \leq 225 \text{ K}$, impact-flow experiments were no longer performed and instead ice nucleation experiments on unshattered particles were per-

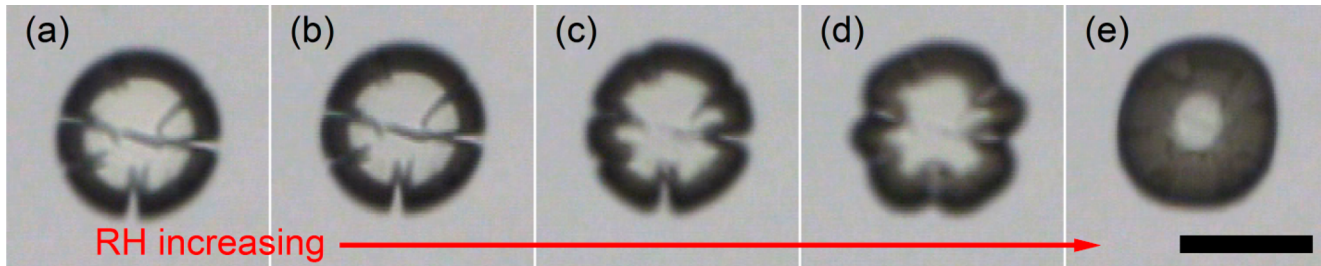


Figure 2. A typical image series of a flow experiment on a shattered methylglyoxal + methylamine aqSOA particle. In this particular experiment, the RH increases from 51 to 93% as the temperature drops from 253.3 to 246.6 K. Initially, as the RH around the shattered particle (a) increases, there is no apparent change in the particle morphology (b). At a set RH, however, the cracks within the particle start to wane and the edges of the particle start to round (c). We have defined this point as RH_{flow} . As the RH is increased beyond RH_{flow} , the particle continues to liquefy (d), eventually attaining a low enough viscosity to form back into near spherical as to reduce the surface tension of the system (e). The size bar in the bottom right-hand corner corresponds to 20 μ m.

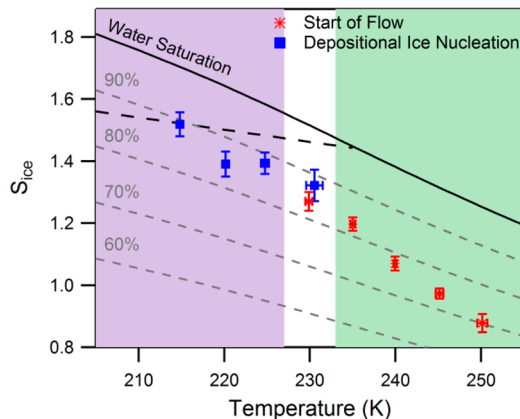


Figure 3. The Start of Flow RH and onset ice saturation ratios for depositional nucleation on methylglyoxal + methylamine aqSOA as a function of temperature. The solid line indicates water saturation (100% RH), and the dashed gray lines correspond to 90, 80, 70, and 60% RH. The dashed black line corresponds to the homogeneous ice nucleation limit.³⁴ For clarity, two regions of different behavior have been shaded. In the green shaded region, the particles liquefy before they can nucleate ice. In the purple shaded region, the particles nucleate ice depositionally before they liquefy. Error bars are reported as one standard deviation.

formed. An example image of ice depositionally nucleating on an aqSOA particle at 220 K can be seen in Figure 4a. To verify that the aqSOA particles were in a nonflowing state, we conducted Raman line maps of ice particles similar to those found in Schill and Tolbert⁸ (not shown). Here, the organic Raman signals (C–H stretching vibrations, $\sim 2900 \text{ cm}^{-1}$) were not observed on the ice crystal that formed. This shows that the

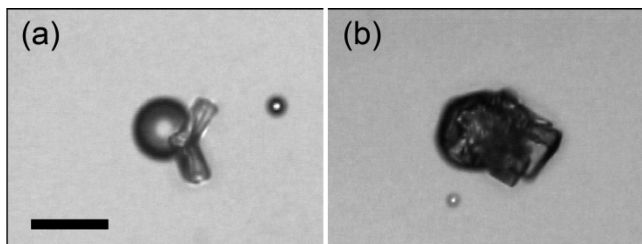


Figure 4. 50 \times images of (a) ice depositionally nucleating on a methylglyoxal + methylamine aqSOA particle and (b) the immersion freezing of aqSOA by AS islands. Both images were taken at 220 K. The size bar in the bottom left-hand corner corresponds to 20 μ m.

aqSOA did not spread out over the growing ice surface and provides further evidence that the particle is in a nonflowing, (semi)solid state at these onset conditions. These ice onset conditions can also be found in Figure 3. As shown, these aqSOA particles require ice supersaturations of $\sim 30\text{--}50\%$, depending on temperature, to nucleate ice.

To study the effect of adding ammonium sulfate to aqSOA, we also performed deliquescence and ice nucleation studies on simulated evaporated cloud droplets that contained 8 mM each of methylglyoxal, methylamine, and ammonium sulfate (aqSOA + AS). As mentioned above, we were unable to conduct impact-flow experiments on these particles because a crystalline phase was present, and so particle shattering would provide no additional information on the phase of the organic material. Therefore, for these particles, we conducted deliquescence experiments on the crystalline material instead. Interestingly, the presence of crystalline material suggests that the particles were not sufficiently viscous to inhibit efflorescence; we attribute this to the plasticizing effect of the inorganic sulfate, which will be discussed later in the manuscript. It is important to note that small α -dicarbonyls have also been shown to react with ammonium ions. This may also contribute to the change in viscosity; however, these reactions produce similar light absorbing and oligomeric molecules as methylglyoxal + methylamine aqSOA.^{26–28} A typical image series of a deliquescence experiment on aqSOA + AS can be seen in Figure 5, and the full video can be found in the Supporting Information (Movie S2). Through the course of this particular experiment, the RH increases from 49 to 88% as the temperature drops from 254.1 to 247.3 K. At low RH, it appears that the particle is in a core–shell configuration (Figure 5a). We have also taken a 2D Raman map of another representative particle under similar conditions (Figure S2). The Raman map also suggests that these particles appear to consist of an ammonium sulfate core with a very thin organic shell. As the RH increases, however, several visual clues unveil the true morphology of these particles. First, the organic shell takes up water, revealing that the ammonium sulfate core is not one particle but many small particles (Figure 5b) embedded in an organic matrix. We will refer to these particles as AS islands from now on. As the organic continues to take up water, the viscosity of the matrix decreases, which allows the AS islands to diffuse throughout the particle (Figure 5c). Eventually, the AS islands undergo prompt deliquescence (Figure 5d). Above this deliquescence point, the particle is visually a homogeneous aqueous solution of aqSOA and ammonium sulfate (Figure 5e).

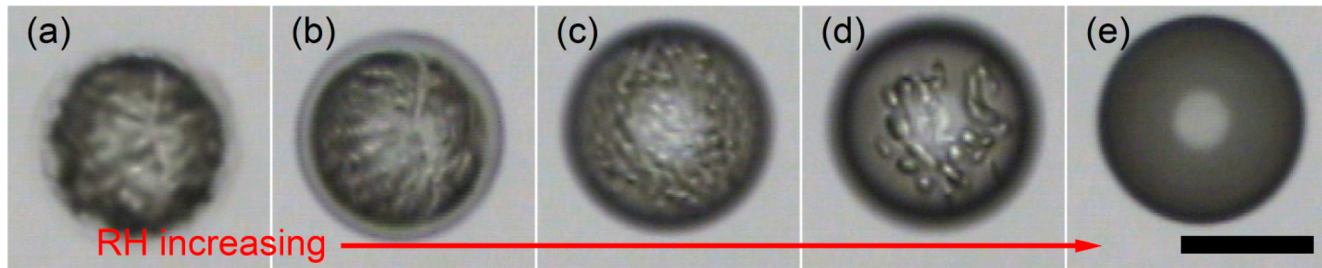


Figure 5. A typical image series of a deliquescence experiment on methylglyoxal + methylamine aqSOA + AS. In this particular experiment, the RH increases from 49 to 88% as the temperature drops from 254.1 to 247.3 K. Initially, the particle looks to be in an effloresced AS core-organic shell morphology (a). As the RH is increased around the particle, the glassy shell takes up water and reveals that the AS core is not one consolidated crystal but many AS islands (b). As the organic matrix liquefies, the AS islands are free to diffuse throughout the particle (c). At a set RH, the AS islands promptly deliquesce (d), turning into a homogeneous aqueous organic-sulfate particle (e). The size bar in the lower right-hand corner corresponds to 20 μm .

Thus, for these mixed particles, the phase progression of the particle upon humidification can be summarized as follows: compact AS islands in a glassy shell, AS islands in a liquid organic matrix, and then fully deliquesced particles. These deliquescence relative humidities (DRH) are shown in Figure 6. As shown, the DRH at all of the temperatures explored is 78

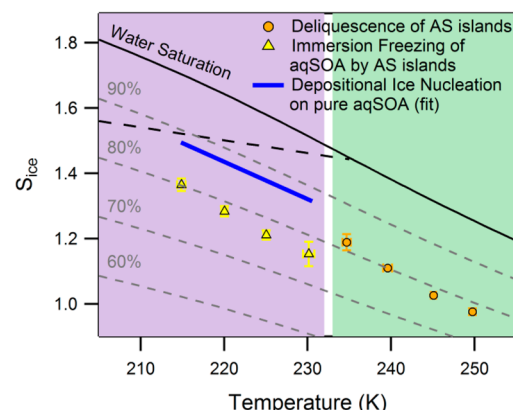


Figure 6. The deliquescence RH of AS islands in a liquid methylglyoxal + methylamine aqSOA matrix and the onset ice saturation ratios for immersion mode nucleation of methylglyoxal + methylamine aqSOA by AS islands as a function of temperature. For comparison, a fit for depositional ice nucleation on pure methylglyoxal + methylamine aqSOA data shown in Figure 3 has been added. The solid line indicates water saturation (100% RH), and the dashed gray lines correspond to 90, 80, 70, and 60% RH. The dashed black line corresponds to the homogeneous ice nucleation limit. For clarity, two regions of different behavior have been shaded. In the green shaded region, the AS islands deliquesce before they can nucleate ice. In the purple shaded region, the AS islands nucleate ice in the immersion mode before they can fully deliquesce. Error bars are reported as one standard deviation.

$\pm 2\%$; thus, the liquid aqSOA does not seem to affect the DRH of ammonium sulfate. An additional discussion concerning liquid–liquid phase separation and efflorescence can be found in the Supporting Information.

At 230 K, we could no longer measure the deliquescence relative humidity of the AS islands because they nucleated ice first. Since the islands are immersed in an aqueous organic matrix, these particles are nucleating ice in the immersion mode. An example image of the immersion freezing of the aqSOA matrix by AS islands at 220 K can be seen in Figure 4b. The onset conditions for ice nucleation by the AS islands

immersed in an aqSOA matrix are also shown in Figure 6. It is important to note that in all cases, the mode of nucleation was immersion freezing by AS islands and not depositional freezing by the glassy organic shell. This was also verified by taking video of the sublimation process (Movie S3). Here as the ice sublimes, we see that the AS islands are contained to the original dimensions of the particle; however, the organic matrix has now spread out with the ice, indicating that it was in a liquid, flowing state at the time of ice nucleation. Upon ice sublimation, however, the organic matrix vitrifies upon drying and converts from a liquid back into a semisolid or glass, leaving an outline of the ice particle (Movie S3). As shown in Figure 6, it can be seen that the supersaturation required for ice nucleation of the aqSOA + AS are lower than for depositional freezing on the pure aqSOA glassy particles. There are two important things to note here: one, adding AS lowers the RH at which the semisolid or glassy aqSOA shell starts to flow. As seen from Figures 3 and 4, from 215 to 235 K, the pure aqSOA can act as a surface for depositional nucleation and be in a nonflowing state at 85–90% RH; by simply adding AS before drying, the aqSOA had turned into an aqueous organic matrix by 75 to 80% RH and could have undergone a humidity induced phase transition at much lower RH. We attribute this to the plasticizing effect of residual inorganic sulfate in the aqSOA matrix; this effect has clearly been seen in the past with both ammonium sulfate and sulfuric acid.^{9,13,15} The second thing to note is that by adding the plasticizer AS to aqSOA, not only does the mode of nucleation change from depositional to immersion, but a result of that is that the particles become more efficient ice nuclei as well.

ATMOSPHERIC IMPLICATIONS

Previously, several studies have looked at the ice nucleation efficiency of single component organic glasses or simple glassy organic mixtures. The first study dedicated to heterogeneous ice nucleation on an organic glass was conducted by Murray et al.¹¹ In that work, the authors found that glassy citric acid required low ice supersaturations, $S_{\text{ice}} = 1.23$, to nucleate ice in the depositional mode. In many of the subsequent studies, single component or simple mixtures of glassy organics were also found to be efficient ice nuclei in the depositional mode.^{12,13} As a result, in one study, it was concluded that organic glasses could compete with ice nucleation on mineral dust particles in midlatitude cirrus clouds.¹²

To the authors' knowledge, the first comprehensive study to probe ice nucleation on complex organics glasses was the study

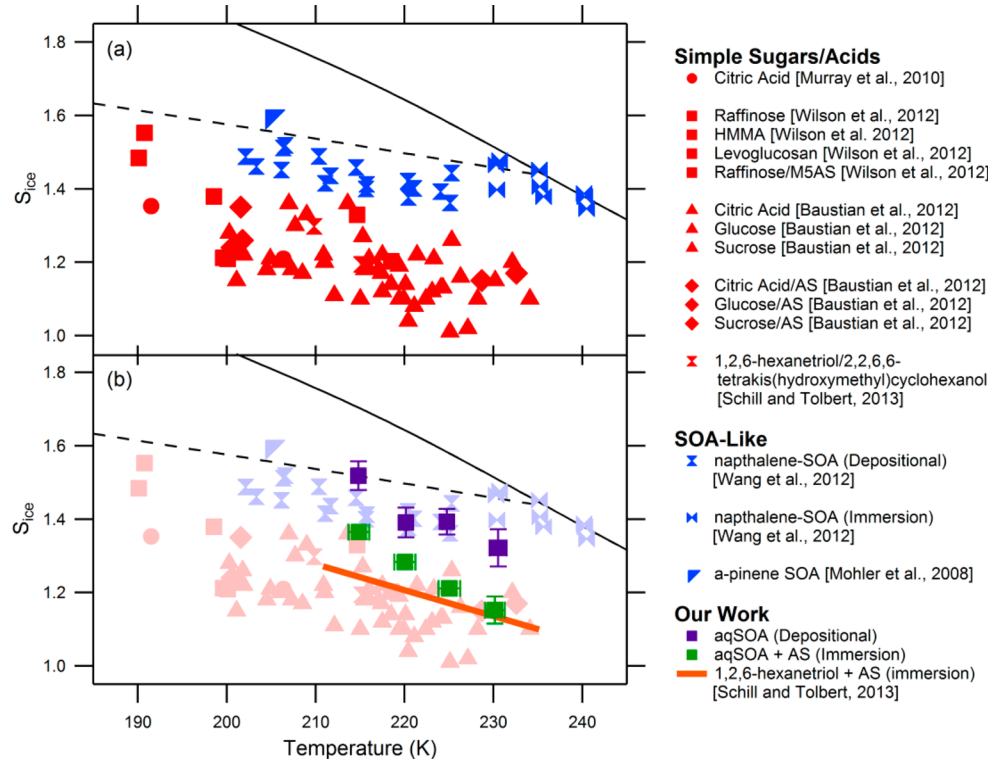


Figure 7. The onset ice saturation ratios for heterogeneous ice nucleation on simple sugar/acid and SOA-like amorphous organic (semi)solids (a) and heterogeneous ice nucleation on methylglyoxal + methylamine aqSOA and immersion freezing of aqSOA by AS islands (b). For comparison, a fit for immersion freezing of the liquid organic 1,2,6-hexanetriol by AS has been added. The solid and dashed black lines correspond to water saturation and the Koop homogeneous freezing line,³⁴ respectively. As shown, the ice nucleation behavior of amorphous organic (semi)solids can be split up into two coarse fractions: simple sugar/acid amorphous organic (semi)solids (red markers) tend to be efficient IN, while SOA-like amorphous (semi)solids (blue markers) tend to require higher supersaturations to nucleate ice. Our results for methylglyoxal + methylamine aqSOA are in agreement with this general trend, while adding AS to the aqSOA tends to change the mode of nucleation and increase the ice nucleation efficacy of the particles. Error bars in the present data are reported as one standard deviation.

by Wang et al.¹⁴ In that work, they found that secondary organic aerosol made from the chamber oxidation of naphthalene could nucleate ice heterogeneously, implying that they are semisolid or glassy. Furthermore, they were able to show that their onset water uptake points coincided with a parametrization for the glass transition line for secondary organic aerosol developed in Koop et al.¹⁰ In contrast to previous studies on single-component glasses, these complex organic glasses required higher ice supersaturations to nucleate ice. In another previous study, Mohler et al.⁷ studied ice nucleation on gasSOA generated from the dark ozonolysis of α -pinene. There, they probed pure gasSOA and saw that it required supersaturations over the Koop homogeneous freezing line to nucleate ice. Unfortunately, the phase of these gasSOA particles was not determined in this particular study. However, several previous works have reported that SOA from the dark ozonolysis of α -pinene can be glassy, according to particle evaporation kinetics^{29,30} as well as particle flow behavior.²⁴ Thus, in the present manuscript, we assume that the gasSOA in the work by Mohler et al.⁷ was in a semisolid or glassy state. Therefore, from the current data, we can generally split the ice nucleation data on amorphous organic (semi)solids into two coarse groups with different ice nucleation properties: "simple sugar/acid" amorphous organic (semi)solids made up of either pure sugars/organic acids or simple mixtures of sugars/organic acids that are generally efficient IN and "SOA-like" amorphous (semi)solids made from the gas-phase oxidation or aqueous-phase reactions of SOA precursors, which are generally poor

IN. This is better seen in Figure 7a. Here, we have color coded the amorphous organic (semi)solids according to these definitions. Simple sugars/organic acids, which consist of six components or less, are color-coded red. In contrast, SOA-like amorphous (semi)solids, which could contain hundreds to thousands of individual components, are color-coded blue. By color coding according to these definitions, it can be seen that simple sugar/acid amorphous organic (semi)solids require lower onset ice saturation ratios to nucleate ice than their SOA-like counterparts. It should be noted that care must be taken when comparing ice nucleation data sets from different techniques; an additional discussion concerning this can be found in the Supporting Information. Nonetheless, although there are only a limited number of studies of ice nucleation on SOA-like systems sampled, Figure 7a suggests that real amorphous organic (semi)solids found in the atmosphere could, in general, be poor IN.

In the present study, we have determined the ice nucleation efficiency of one type of aqSOA, generated from the dark reactions of small aldehydes and amines. Our data is plotted over the previous work in Figure 7b. In concurrence with previous experiments on gasSOA, these (semi)solid aqSOA particles can nucleate ice in the depositional freezing mode but are poor IN. We hypothesize the different ice nucleation behavior of simple sugar/acid and SOA-like amorphous organic (semi)solids may be due to their differences in surface chemistry. The sugars/organic acids shown in Figure 7a are molecules with predominantly alcohol moiety; given that these

particles are amorphous, there is a high likelihood that there are considerable $-OH$ groups at the particle surface. In contrast, the predicted oxygenated products expected to be found in naphthalene gasSOA tend to have more carbonyl moieties than alcohols.¹⁵ Similarly, the major products expected from the dark reaction of methylglyoxal + methylamine in evaporating droplets under the pH conditions in our experiments are imine oligomers,²⁰ which have more carbonyl moieties than alcohol. Previously, it was found that increasing the surface hydrophilicity would increase the ice nucleation efficiency of soot³¹ and crystalline organic particles.³² In the study by Wang et al.,¹⁴ the O:C ratio of the naphthalene gasSOA was determined by the Aerodyne aerosol mass spectrometer. Interestingly, Wang et al. saw no significant difference in ice nucleation efficiency between his low, medium, and high O:C ratio samples, which had values of 0.27, 0.54, and 1.0, respectively. Although there are no explicit mechanisms for the reaction products from the photooxidation of naphthalene in a Potential Aerosol Mass chamber, the results from Saukko et al.¹⁵ suggest that the expected reactions oxygenate naphthalene via the formation of carbonyls and carboxylic acids. Given the evidence above, we believe that not just surface hydrophilicity but surface $-OH$ density may be a large driving force in the ice nucleation efficiency of amorphous organic aerosol. It should be noted that we did not measure the surface $-OH$ density, so these interpretations are speculative. Further, several other parameters vary between these two broadly defined categories that may also be affecting the ice nucleation efficiency.

Finally, our results also show that by adding AS to aqSOA, the viscosity of the aqSOA matrix was lowered due to the plasticizing effect of residual AS in the aqSOA matrix. This allowed the AS to effloresce upon drying, causing AS islands to embed in the aqSOA organic matrix. Upon liquefaction of the aqSOA matrix by humidification of the dried particles, these AS islands could then potentially serve as immersion IN and increase the ice nucleation efficacy of these particles in comparison to depositional ice nucleation on pure aqSOA (Figure 7b). The efficiency of freezing aqueous solutions of organics by AS in the immersion mode is in agreement with a previous study from our group examining the immersion freezing of aqueous 1,2,6-hexanetriol by effloresced AS over a similar temperature range.⁸ At colder temperatures, however, there is a small deviation between the two data sets. Here, ice nucleation on AS islands immersed in methylglyoxal + methylamine aqSOA require slightly higher supersaturations than AS particles coated with 1,2,6-hexanetriol. Identifying the source of this deviation is beyond the scope of this paper, but the authors postulate that the higher super saturations required for the AS islands to freeze the aqSOA matrix could be due to higher viscosity of the matrix and hence slower water diffusion in the aqSOA matrix relative to 1,2,6-hexanetriol.

The plasticizing effect of AS on glassy organic aerosol has been noted in previous publications.^{9,13,15} Thus, although SOA-like glasses may be a poor IN, if a sufficient amount of AS is present such that AS efflorescence is not inhibited,³³ glassy organic-sulfate particles can become efficient IN since the ice nucleation efficiency of AS in the immersion mode is minimally affected by the presence of liquid aqSOA. Finally, changing the mode of ice nucleation also changes the ice crystal habit of the ice particle (Figure 4), which could affect the light scattering properties of ice crystals that nucleated from mixed organic-sulfate particles found in the upper troposphere.

ASSOCIATED CONTENT

Supporting Information

Figures S1 and S2, movies S1–S3, and additional text. This material is available free of charge via the Internet at <http://pubs.acs.org>.

AUTHOR INFORMATION

Corresponding Author

*Phone: 303.492.3177. Fax: 303.492.1149. E-mail: tolbert@colorado.edu.

Notes

The authors declare no competing financial interest.

ACKNOWLEDGMENTS

This work was supported by the National Science Foundation under grants AGS1048536, ATM0650023, and AGS1129002.

REFERENCES

- (1) Forster, P. et al. Changes in atmospheric constituents and radiative forcing. In *Climate Change 2007: The Physical Science Basis*. Contribution of Working Group I to the Fourth Assessment Report of the Intergovernmental Panel on Climate Change. Solomon, S., et al., Eds.; Cambridge Univ. Press: Cambridge, U. K., 2007; pp 131–234.
- (2) Froyd, K. D.; Murphy, D. M.; Sanford, T. J.; Thomson, D. S.; Wilson, J. C.; Pfister, L.; Lait, L. Aerosol composition of the tropical upper troposphere. *Atmos. Chem. Phys.* **2009**, *9* (13), 4363–4385.
- (3) Froyd, K. D.; Murphy, D. M.; Lawson, P.; Baumgardner, D.; Herman, R. L. Aerosols that form subvisible cirrus at the tropical tropopause. *Atmos. Chem. Phys.* **2010**, *10* (1), 209–218.
- (4) Abbatt, J. P. D.; Benz, S.; Cziczo, D. J.; Kanji, Z.; Lohmann, U.; Mohler, O. Solid ammonium sulfate aerosols as ice nuclei: A pathway for cirrus cloud formation. *Science* **2006**, *313* (5794), 1770–1773.
- (5) Wise, M. E.; Baustian, K. J.; Tolbert, M. A. Internally mixed sulfate and organic particles as potential ice nuclei in the tropical tropopause region. *Proc. Natl. Acad. Sci. U. S. A.* **2010**, *107* (15), 6693–6698.
- (6) Baustian, K. J.; Wise, M. E.; Tolbert, M. A. Depositional ice nucleation on solid ammonium sulfate and glutaric acid particles. *Atmos. Chem. Phys.* **2010**, *10* (5), 2307–2317.
- (7) Mohler, O.; Benz, S.; Saathoff, H.; Schnaiter, M.; Wagner, R.; Schneider, J.; Walter, S.; Ebert, V.; Wagner, S. The effect of organic coating on the heterogeneous ice nucleation efficiency of mineral dust aerosols. *Environ. Res. Lett.* **2008**, *3*, (2).
- (8) Schill, G. P.; Tolbert, M. A. Heterogeneous ice nucleation on phase-separated organic-sulfate particles: effect of liquid vs. glassy coatings. *Atmos. Chem. Phys.* **2013**, *13* (9), 4681–4695.
- (9) Zobrist, B.; Marcolla, C.; Pedernera, D. A.; Koop, T. Do atmospheric aerosols form glasses? *Atmos. Chem. Phys.* **2008**, *8* (17), 5221–5244.
- (10) Koop, T.; Bookhold, J.; Shiraiwa, M.; Poschl, U. Glass transition and phase state of organic compounds: dependency on molecular properties and implications for secondary organic aerosols in the atmosphere. *Phys. Chem. Chem. Phys.* **2011**, *13* (43), 19238–19255.
- (11) Murray, B. J.; Wilson, T. W.; Dobbie, S.; Cui, Z. Q.; Al-Jumur, S.; Mohler, O.; Schnaiter, M.; Wagner, R.; Benz, S.; Niemand, M.; Saathoff, H.; Ebert, V.; Wagner, S.; Karcher, B. Heterogeneous nucleation of ice particles on glassy aerosols under cirrus conditions. *Nat. Geosci.* **2010**, *3* (4), 233–237.
- (12) Wilson, T. W.; Murray, B. J.; Wagner, R.; Möhler, O.; Saathoff, H.; Schnaiter, M.; Skrotzki, J.; Price, H. C.; Malkin, T. L.; Dobbie, S.; Al-Jumur, S. M. R. K. Glassy aerosols with a range of compositions nucleate ice heterogeneously at cirrus temperatures. *Atmos. Chem. Phys. Discuss.* **2012**, *12* (4), 8979–9033.
- (13) Baustian, K. J.; Wise, M. E.; Jensen, E. J.; Schill, G. P.; Freedman, M. A.; Tolbert, M. A. State transformations and ice

- nucleation in amorphous (semi-)solid organic aerosol. *Atmos. Chem. Phys.* **2013**, *13* (11), 5615–5628.
- (14) Wang, B.; Lambe, A. T.; Massoli, P.; Onasch, T. B.; Davidovits, P.; Worsnop, D. R.; Knopf, D. A. The deposition ice nucleation and immersion freezing potential of amorphous secondary organic aerosol: Pathways for ice and mixed-phase cloud formation. *J. Geophys. Res.* **2012**, *117* (D16), D16209.
- (15) Saukko, E.; Lambe, A. T.; Massoli, P.; Koop, T.; Wright, J. P.; Croasdale, D. R.; Pedernera, D. A.; Onasch, T. B.; Laaksonen, A.; Davidovits, P.; Worsnop, D. R.; Virtanen, A. Humidity-dependent phase state of SOA particles from biogenic and anthropogenic precursors. *Atmos. Chem. Phys.* **2012**, *12* (16), 7517–7529.
- (16) Blando, J. D.; Turpin, B. J. Secondary organic aerosol formation in cloud and fog droplets: a literature evaluation of plausibility. *Atmos. Environ.* **2000**, *34* (10), 1623–1632.
- (17) Ervens, B.; Turpin, B. J.; Weber, R. J. Secondary organic aerosol formation in cloud droplets and aqueous particles (aqSOA): a review of laboratory, field and model studies. *Atmos. Chem. Phys.* **2011**, *11* (21), 11069–11102.
- (18) De Haan, D. O.; Tolbert, M. A.; Jimenez, J. L. Atmospheric condensed-phase reactions of glyoxal with methylamine. *Geophys. Res. Lett.* **2009**, *36*.
- (19) De Haan, D. O.; Hawkins, L. N.; Kononenko, J. A.; Turley, J. J.; Corrigan, A. L.; Tolbert, M. A.; Jimenez, J. L. Formation of nitrogen-containing oligomers by methylglyoxal and amines in simulated evaporating cloud droplets. *Environ. Sci. Technol.* **2011**, *45* (3), 984–991.
- (20) Sedehi, N.; Takano, H.; Blasic, V. A.; Sullivan, K. A.; De Haan, D. O. Temperature- and pH-dependent aqueous-phase kinetics of the reactions of glyoxal and methylglyoxal with atmospheric amines and ammonium sulfate. *Atmos. Environ.* **2013**, *77* (0), 656–663.
- (21) Murphy, D. M.; Koop, T. Review of the vapour pressures of ice and supercooled water for atmospheric applications. *Q. J. R. Meteorol. Soc.* **2005**, *131* (608), 1539–1565.
- (22) Murray, B. J.; Haddrell, A. E.; Peppe, S.; Davies, J. F.; Reid, J. P.; O'Sullivan, D.; Price, H. C.; Kumar, R.; Saunders, R. W.; Plane, J. M. C.; Umo, N. S.; Wilson, T. W. Glass formation and unusual hygroscopic growth of iodine acid solution droplets with relevance for iodine mediated particle formation in the marine boundary layer. *Atmos. Chem. Phys.* **2012**, *12* (18), 8575–8587.
- (23) Greenspan, L. Humidity fixed-points of binary saturated aqueous-solutions. *J. Res. Natl. Bur. Stand., Sect. A* **1977**, *81* (1), 89–96.
- (24) Renbaum-Wolff, L.; Grayson, J. W.; Bateman, A. P.; Kuwata, M.; Sellier, M.; Murray, B. J.; Shilling, J. E.; Martin, S. T.; Bertram, A. K. Viscosity of α -pinene secondary organic material and implications for particle growth and reactivity. *Proc. Natl. Acad. Sci.* **2013**, *110* (20), 8014–8019.
- (25) Karcher, B.; Strom, J. The roles of dynamical variability and aerosols in cirrus cloud formation. *Atmos. Chem. Phys.* **2003**, *3*, 823–838.
- (26) Yu, G.; Bayer, A. R.; Galloway, M. M.; Korshavn, K. J.; Fry, C. G.; Keutsch, F. N. Glyoxal in aqueous ammonium sulfate solutions: Products, kinetics and hydration effects. *Environ. Sci. Technol.* **2011**, *45* (15), 6336–6342.
- (27) Sareen, N.; Schwier, A. N.; Shapiro, E. L.; Mitroo, D.; McNeill, V. F. Secondary organic material formed by methylglyoxal in aqueous aerosol mimics. *Atmos. Chem. Phys.* **2010**, *10* (3), 997–1016.
- (28) Noziere, B.; Dziedzic, P.; Cordova, A. Products and kinetics of the liquid-phase reaction of glyoxal catalyzed by ammonium ions (NH_4^+). *J. Phys. Chem. A* **2009**, *113* (1), 231–237.
- (29) Vaden, T. D.; Imre, D.; Beranek, J.; Shrivastava, M.; Zelenyuk, A. Evaporation kinetics and phase of laboratory and ambient secondary organic aerosol. *Proc. Natl. Acad. Sci. U. S. A.* **2011**, *108* (6), 2190–2195.
- (30) Cappa, C. D.; Wilson, K. R. Evolution of organic aerosol mass spectra upon heating: implications for OA phase and partitioning behavior. *Atmos. Chem. Phys.* **2011**, *11* (5), 1895–1911.
- (31) Gorbunov, B.; Baklanov, A.; Kakutkina, N.; Windsor, H. L.; Toumi, R. Ice nucleation on soot particles. *J. Aerosol Sci.* **2001**, *32* (2), 199–215.
- (32) Schill, G. P.; Tolbert, M. A. Depositional ice nucleation on monocarboxylic acids: Effect of the O:C ratio. *J. Phys. Chem. A* **2012**, *116* (25), 6817–6822.
- (33) Bodsworth, A.; Zobrist, B.; Bertram, A. K. Inhibition of efflorescence in mixed organic-inorganic particles at temperatures less than 250 K. *Phys. Chem. Chem. Phys.* **2010**, *12* (38), 12259–12266.
- (34) Koop, T.; Luo, B. P.; Tsias, A.; Peter, T. Water activity as the determinant for homogeneous ice nucleation in aqueous solutions. *Nature* **2000**, *406* (6796), 611–614.